Published in final edited form as:
Nano Lett. 2011 October 12; 11(10): 4411–4414. doi:10.1021/nl2025882.

Nanoparticles for targeting the infarcted heart

Tal Dvir[1,2,*], **Michael Bauer**[3,*], **Avi Schroeder**[1], **Jonathan H. Tsui**[2], **Daniel G. Anderson**[1], **Robert Langer**[1], **Ronglih Liao**[3,†], and **Daniel S. Kohane**[2,†]

[1]Department of Chemical Engineering, Massachusetts Institute of Technology, Cambridge, MA 02139

[2]Laboratory for Biomaterials and Drug Delivery, Department of Anesthesiology, Division of Critical Care Medicine, Children's Hospital Boston, Harvard Medical School, 300 Longwood Avenue, Boston, Massachusetts 02115

[3]Cardiovascular Division, Department of Medicine, Brigham and Women's Hospital, Harvard Medical School, Boston, MA 02115

Abstract

We report a nanoparticulate system capable of targeting the heart after myocardial infarction (MI). Targeting is based on overexpression of angiotensin II type 1 receptor (AT1) in the infarcted heart. Liposomes 142 nm in diameter were conjugated with a ligand specific to AT1. The nanoparticles were able to specifically target cardiac cells in vitro, and in the infarcted heart after intravenous injection *in vivo*. This system may be useful for delivering therapeutic agents specifically to the infarcted heart.

Keywords

Liposomes; Myocardial infarction; Nanoparticles; Targeting

Coronary artery disease can lead to myocardial ischemia and/or myocardial infarction (MI), the leading cause of morbidity and mortality in the USA[1]. Since cardiomyocytes are terminally differentiated and cannot proliferate, and given that the number of stem cells in the heart is limited, the heart cannot regenerate, leading to chronic cardiac dysfunction. Approximately 50% of patients who have had a first MI will die within the next 5 years[1]. The only cure for these end-stage patients is cardiac transplantation. As cardiac donors are scarce, there is an urgent need to develop new strategies that will promote heart regeneration.

Many experimental approaches to treating the infarcted heart involve supplying growth factors, cytokines, drugs and other biomolecules to the dying cells in the scar tissue[2]. These therapeutic agents have been delivered by direct injection, or by injecting biomolecule-loaded microparticles or gels to the LV[3–8]. However, the efficacy of these approaches may be hampered by lack of retention of the factors or microparticles in the desired area. An alternative extant approach is transplantation of biomaterials capable of releasing biomolecules into the scar tissue microenvironment[9–11]. This strategy involves surgery, with its attendant risks and costs.

[†]To whom correspondence should be addressed: rliao@rics.bwh.harvard.edu or Daniel.Kohane@childrens.harvard.edu.
[*]Equal contribution

Targeted nanoparticles provide an attractive approach as they may be injected intravenously (IV), circulate in the body for long periods and only bind at desired organs. Recent studies have successfully demonstrated selective targeting of engineered nanoparticles to tumors 12, 13 and the feasibility of such targeting systems has already been demonstrated clinically [14]. In the infarcted heart micro- and nanoparticles have been used to target macrophages[15] and blood vessels[16].

In order to develop a successful targeting system, researchers must overcome two main barriers on the pathway between the circulatory and the target cells. First, the transfer of the delivery system across the normal vascular endothelium is difficult. Nanoparticles can cross endothelia more readily in circumstances where the vasculature is abnormal or disrupted, as in tumors – a process referred to as enhanced permeation and retention (EPR). Second, if active targeting is desired, it is important to identify a molecular target at the desired site of drug action that is substantially enriched relative to the rest of the body, and a ligand to that target.

The technology reported in this paper relies on two main observations. First, after MI the blood vessels in the LV become leaky[17]; this may allow penetration of nano-sized particles in a manner analogous to EPR. Secondly, it has recently been shown that the AT1 receptor is overexpressed in the infarcted heart[18] and thus may serve as a target.

To verify that AT1 receptor overexpression occurs after hypoxia as after MI, we exposed isolated cardiac cells to low oxygen levels (48 h at 5% O_2). The cells were then fixed and stained with antibodies against the AT1 receptor. A three-fold increase in the expression of the AT1 receptor ($p = 0.0009$) was observed in cells subjected to hypoxia compared to cells grown under normal conditions (Figure 1A and B). This phenomenon was also observed in vivo after LV MI induced by occlusion of the left coronary artery. Cells located in the LV expressed higher AT1 receptor levels than those of the infarcted heart right ventricle or normal LV (Figure 1C-E).

We designed a nanoparticulate system that could specifically target cardiac cells based on this phenomenon (Figure 2). The system comprised a vehicle and a targeter. The vehicle was a nano-sized PEGylated liposome (142 ± 8 nm) that could carry a therapeutic payload (e.g. growth factors, cytokines etc.) and release them in a controlled manner. The targeter was composed of the amino acid sequence Gly-Gly-Gly-Gly-Asp-Arg-Val-Tyr-Ile-His-Pro-Phe (the AT1 receptor targeter), where the 4 glycine residues served as a spacer and the remaining 8 amino acids are the amino acid sequence of angiotensin II[19]. This peptide was covalently attached to the carboxylic groups on the PEGylated liposomes to form a nanoparticulate system able to target the infarcted heart (referred to henceforth as AT1 nanoparticles).

To investigate the potential of the AT1 nanoparticles to bind cardiac cells we isolated cardiac cells as previously described[20] and cultured them in 8-well chamber slides (2.5×10^5 per well) for 48 h. Twenty μL of AT1 nanoparticles (~1.5×10^{14} particles/mL) containing fluorescent dye were cultured with the cells for 30 min. The medium was removed and the cultures were carefully washed. To demonstrate AT1 targeter specificity, these particles were compared to others bearing a targeter with the same amino acids in a scrambled order. AT1 particles showed greater targeting ability (Figure 3A and B). After 30 min, 52% of the cells incubated with AT1 nanoparticles were targeted in comparison to only 27% of the cardiac cells incubated with the scrambled particles ($p = 0.0003$). When cells were subjected to 48 h of hypoxia (5%), the proportion of targeted cells rose from 52% to more than 83% ($p = 0.007$) (Figure 3C–E).

We demonstrated the potential of AT1 nanoparticles to target the infarcted heart in mice in which MIs were induced by ligation of the left descending coronary artery. Fluorescently labeled nanoparticles (AT1 or scrambled peptide) were injected into the right jugular vein 1, 4 and 7 days after MI. We allowed the nanoparticles to circulate in the body for 24 h before sacrificing the animals. The hearts were isolated and immediately imaged using an in vivo imaging system (IVIS) and the signal intensity was measured. As shown by the representative pictures of the isolated hearts, the particles accumulated mainly in the left ventricle (Figure 4A). Thin sections of the LV wall after MI further validated that the particles were present in the LV (Figure 4B). Quantification of the fluorescence in the hearts revealed statistically significantly higher levels of AT1 nanoparticles compared to scrambled particles on days 1 ($p = 0.05$) and 7 ($p = 0.02$) post infarction (Figure 4C). To ensure that the binding we obtain after MI is specific to injured hearts and does not occur in healthy animals we injected AT1 or scrambled nanoparticles into sham-operated mice (i.e. animals without coronary occlusion). There was negligible binding in these LVs (Figure S1). The amounts of AT1 nanoparticles accumulated in the infarcted heart on days 1, 4, and 7 were 48, 39, and 27% percent of the total amount accumulated in all organs studied respectively (Figure S2). The differences in accumulation over time may be attributable to concurrent changes in inflammation, perfusion, and vascularization after infarction.

In conclusion, we report two principal findings. First, nanoparticles will target the injured but not the healthy heart, suggesting that this could be an approach that could be exploited for drug delivery after MI, in a manner analogous to the way in way in which nanoparticles are used to preferentially but passively target tumors[21]. Second, AT1 targeting further enhanced delivery to the injured myocardium. Both approaches could be used to reduce systemic toxicity of delivered drugs and – most importantly – increase local therapeutic effect. Decreasing particle size and optimizing targeter density could further increase targeting efficiency. These systems could provide sustained release of bioactive molecules specifically to the infarcted heart and promote cardiac tissue regeneration. Many biomolecules have been reported to have a therapeutic effect on the infarcted heart. For example, microparticles containing a p38 inhibitor injected directly to the infarcted heart were able to reduce the fibrotic area[3]. Furthermore, the release of insulin-like growth factor[5], hepatocyte growth factor[5], platelet-derived growth factor[4], stromal-cell-derived growth factors[22] or periostin[23] in close proximity to cardiac infarcts was able to attenuate the deterioration of the LV. These nanoparticulate formulations have the advantage of being delivered intravenously, obviating the need for cardiac catheterization or other surgical procedures.

Experimental section

Cardiac cell isolation

Ventricular myocytes were isolated from neonatal (1- 2 d) Sprague-Dawley rats as previously described[20] using 6 to 7 cycles of enzyme digestion Isolated ventricles were cut to approximately $1mm^3$ pieces and incubated (37°C, 30 min) repeatedly (6–7 times) in buffer with Collagenase type II (95 U/mL; Worthington, Lakewood, NJ) and pancreatin (0.6 mg/mL; Sigma, St Louis, MO). After each digestion round, the mixture was centrifuged (600 g, 5 min, 25°C), and the cell pellet was re-suspended in cold M-199 medium supplemented with 5% FBS (Invitrogen, Carlsbad, CA).

Immunostaining

Immunofluorescence staining was performed as described [24] In brief, samples were fixed and permeabilized in cold methanol, blocked for 1 hour at room temperature in PBS containing 2% serum. After three buffer washes, the samples were incubated for 1 hour with

antibodies to β-actin (FITC-conjugated, Sigma), AT1 (Abcam, Cambridge, MA) or sarcomeric actinin (Invitrogen). The samples were incubated for additional 1 hour with goat anti-mouse Alexa conjugated antibodies (Sigma). For nuclear detection, the cells were incubated for 3 minutes with Hoechst 33258 (Sigma) and washed. Imaging was performed with an inverted Zeiss fluorescence microscope model Axiovert 200M and analysis was performed using AxioVision 4.5. Images were quantitated using Image J software (NIH).

Liposome preparation and targeter conjugation

L-α-phosphatidylcholine (HSPC), Mw 762.1, (Avanti Polar Lipids, Alabaster, AL) 1,2-distearoyl-*sn*-glycero-3-phosphoethanolamine-N-[carboxy(polyethylene glycol)-2000], Mw 2849.5, (Avanti) and cholesterol (Sigma), in a mole ratio of 67.9:2.4:29.7, respectively, were dissolved in absolute ethanol at 62–65°C. The lipid solution was hydrated in an aqueous solution containing a fluorescent probe (DyLight 649, Thermo Scientific, lipid conc. 40.4 mg/mL, dye conc. 0.4 mg/mL) to form multilamellar vesicles. The multilamellar vesicles were downsized by stepwise extrusion through polycarbonate membranes (Osmonics, Trevose, PA) using a Lipex extruder (Northern Lipids, Vancouver, Canada) starting at a pore diameter of 400 nm and ending at 100 nm. Non-encapsulated dye was removed by dialysis against PBS using 10^6 MW cut-off cellulose ester tubing (Spectra/Por Biotech, Ranco Domingues, CA). A mean particle diameter of 142 ± 8 nm was measured by dynamic light scattering. Conjugation of the targeter was performed as described[25]. In brief, five mL of liposome solution (~1.5×10^{14}/mL) were incubated with 20 mg of 1-(3-dimethylaminopropyl)-3-ethylcarbodimide hydrochloride (EDC, Sigma) and 40 mg of sulfo-N-hydroxysuccinimide (NHS, Sigma) for 2.5 hours at room temperature with gentle stirring. The resulting NHS-activated particles were covalently linked to 4 mg NH2-GGGGYDRVTIHPF-NH2 or the scrambled peptide NH2-GGGGFHPDYRVI-NH2 (GenScript Corp., Piscataway, NJ) over-night at room temperature with gentle stirring.

Assessment of cell targeting in vitro

Cardiac cell targeting was assessed as described[25]. In brief, on the day of experiments, cells were washed with pre-warmed PBS and incubated with pre-warmed media with addition of nanoparticles. The cultured were washed with PBS three times, fixed and stained. The number of targeted cells was quantified by fluorescent microscopy at 20X magnification and divided by the total cell number. All measurements were averaged over 3 consecutive images within every well ($n \geq 6$).

Mouse model of MI and nanoparticle injection

MI was induced as described[26]. C57/BL6 female mice were anesthetized (IP injection) with a combination of ketamine (40 mg/kg) and xylazine (10 mg/kg), intubated, and mechanically ventilated. The chest was opened by left thoracotomy, the pericardium was removed, and the proximal left coronary artery was permanently occluded with an intramural stitch. One, 4, and 7 days post-MI, nanoparticles (100 μL) were injected into the right jugular vein. Twenty-four hours post-injection, the mice were sacrificed and their hearts were taken for evaluation. All animal procedures were approved by the Institutional Animal Care and Use Committee of the Harvard Medical School.

Assessment of cell targeting in vivo

Isolated heart (n= 4 for each time point) imaging was performed with an IVIS Spectrum measurement system (Xenogen, Hopkinton, MA, USA). Fluorescent images were captured at an excitation wavelength of 605 nm and emission wavelength of 720 nm under optimized imaging configurations. Data were analyzed using the manufacturer's Living Image 3.1 software.

Statistical analysis

Data are presented as means ± S.D. Univariate differences between the groups were assessed with Student's t test. All analyses were performed using GraphPad Prism version 5.00 for Windows (GraphPad Software, San Diego, CA). $p < 0.05$ was considered statistically significant.

Supplementary Material

Refer to Web version on PubMed Central for supplementary material.

Acknowledgments

This research was funded by NIH Grants EB000244, EB006365 (to R. Langer), HL 086967 (to R. Liao), and GM073626 (to D.S.K.). T.D. and M.B. acknowledge Postdoctoral Fellowships from the American Heart Association. A.S. acknowledges a Postdoctoral Fellowship from the Misrock Foundation.

References

1. American Heart Association. 2006
2. Ruvinov E, Dvir T, Leor J, Cohen S. Myocardial repair: from salvage to tissue reconstruction. Expert Rev Cardiovasc Ther. 2008; 6:669–686. [PubMed: 18510484]
3. Sy JC, et al. Sustained release of a p38 inhibitor from non-inflammatory microspheres inhibits cardiac dysfunction. Nat Mater. 2008; 7:863–868. [PubMed: 18931671]
4. Hsieh PC, Davis ME, Gannon J, MacGillivray C, Lee RT. Controlled delivery of PDGF-BB for myocardial protection using injectable self-assembling peptide nanofibers. J Clin Invest. 2006; 116:237–248. [PubMed: 16357943]
5. Ruvinov E, Leor J, Cohen S. The effects of controlled HGF delivery from an affinity-binding alginate biomaterial on angiogenesis and blood perfusion in a hindlimb ischemia model. Biomaterials. 31:4573–4582. [PubMed: 20206988]
6. Ruvinov E, Leor J, Cohen S. The promotion of myocardial repair by the sequential delivery of IGF-1 and HGF from an injectable alginate biomaterial in a model of acute myocardial infarction. Biomaterials. 32:565–578. [PubMed: 20889201]
7. Garbern JC, Minami E, Stayton PS, Murry CE. Delivery of basic fibroblast growth factor with a pH-responsive, injectable hydrogel to improve angiogenesis in infarcted myocardium. Biomaterials. 32:2407–2416. [PubMed: 21186056]
8. Yockman JW, et al. Polymeric gene delivery of ischemia-inducible VEGF significantly attenuates infarct size and apoptosis following myocardial infarct. Gene Ther. 2009; 16:127–135. [PubMed: 18784748]
9. Dvir T, et al. Prevascularization of cardiac patch on the omentum improves its therapeutic outcome. Proc Natl Acad Sci U S A. 2009; 106:14990–14995. [PubMed: 19706385]
10. Fitzpatrick JR 3rd, et al. Tissue-engineered pro-angiogenic fibroblast scaffold improves myocardial perfusion and function and limits ventricular remodeling after infarction. J Thorac Cardiovasc Surg. 140:667–676. [PubMed: 20363480]
11. Miyagi Y, et al. Surgical ventricular restoration with a cell- and cytokine-seeded biodegradable scaffold. Biomaterials. 31:7684–7694. [PubMed: 20659765]
12. Mallidi S, et al. Multiwavelength photoacoustic imaging and plasmon resonance coupling of gold nanoparticles for selective detection of cancer. Nano Lett. 2009; 9:2825–2831. [PubMed: 19572747]
13. Farokhzad OC, et al. Targeted nanoparticle-aptamer bioconjugates for cancer chemotherapy in vivo. Proc Natl Acad Sci U S A. 2006; 103:6315–6320. [PubMed: 16606824]
14. von Mehren M, Adams GP, Weiner LM. Monoclonal antibody therapy for cancer. Annu Rev Med. 2003; 54:343–369. [PubMed: 12525678]

15. Harel-Adar T, et al. Modulation of cardiac macrophages by phosphatidylserine-presenting liposomes improves infarct repair. Proceedings of the national academy of science USA. 2011; 108:1827–1832.

16. Scott RC, et al. Targeting VEGF-encapsulated immunoliposomes to MI heart improves vascularity and cardiac function. FASEB Journal. 2009; 23:3361–3367. [PubMed: 19535683]

17. Weis SM. Vascular permeability in cardiovascular disease and cancer. Curr Opin Hematol. 2008; 15:243–249. [PubMed: 18391792]

18. Molavi B, Chen J, Mehta JL. Cardioprotective effects of rosiglitazone are associated with selective overexpression of type 2 angiotensin receptors and inhibition of p42/44 MAPK. Am J Physiol Heart Circ Physiol. 2006; 291:H687–693. [PubMed: 16582019]

19. Greene LJ, Spadaro AC, Martins AR, Perussi De Jesus WD, Camargo AC. Brain endo-oligopeptidase B: a post-proline cleaving enzyme that inactivates angiotensin I and II. Hypertension. 1982; 4:178–184. [PubMed: 6175571]

20. Dvir T, Benishti N, Shachar M, Cohen S. A novel perfusion bioreactor providing a homogenous milieu for tissue regeneration. Tissue Eng. 2006; 12:2843–2852. [PubMed: 17518653]

21. Peer D, et al. Nanocarriers as an emerging platform for cancer therapy. Nat Nanotechnol. 2007; 2:751–760. [PubMed: 18654426]

22. Segers VF, et al. Local delivery of protease-resistant stromal cell derived factor-1 for stem cell recruitment after myocardial infarction. Circulation. 2007; 116:1683–1692. [PubMed: 17875967]

23. Kuhn B, et al. Periostin induces proliferation of differentiated cardiomyocytes and promotes cardiac repair. Nat Med. 2007; 13:962–969. [PubMed: 17632525]

24. Dvir T, Levy O, Shachar M, Granot Y, Cohen S. Activation of the ERK1/2 cascade via pulsatile interstitial fluid flow promotes cardiac tissue assembly. Tissue Eng. 2007; 13:2185–2193. [PubMed: 17518740]

25. Dvir T, Banghart MR, Timko BP, Langer R, Kohane DS. Photo-targeted nanoparticles. Nano Lett. 2010; 10:250–254. [PubMed: 19904979]

26. Bauer M, et al. Echocardiographic speckle-tracking based strain imaging for rapid cardiovascular phenotyping in mice. Circ Res. 2011; 108:908–916. [PubMed: 21372284]

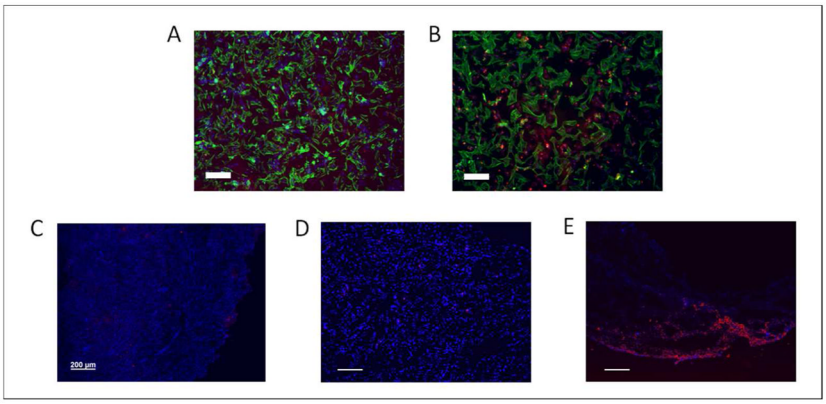

Figure 1.

AT1 expression in normal and diseased conditions. A, B. in vitro assessment of AT1 receptor expression. A. Cardiomyocytes cultured under normal conditions. B. Cardiomyocytes cultured under hypoxic conditions (48 h, 5 % O2). C. Expression of AT1 in vivo in the LV of the pristine heart. D, E, Expression of AT1 in vivo 7 days post MI. D. Expression in the right ventricle. E. Expression in the LV in the infarcted area. Green: β-actin, red: AT1, blue: nuclei. Bar = 200 μm. 207×99mm (150 × 150 DPI)

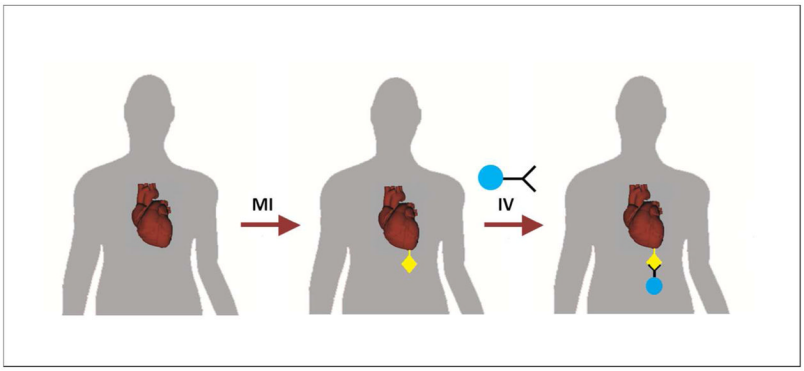

Figure 2.

Concept schematic. After myocardial infarction, the AT1 receptor is overexpressed in the LV. Nanoparticles conjugated with a ligand specific for the AT1 receptor are injected intravenously. After circulating in the body the particles specifically target the LV, where they can release therapeutic agents. 267×121mm (150 × 150 DPI)

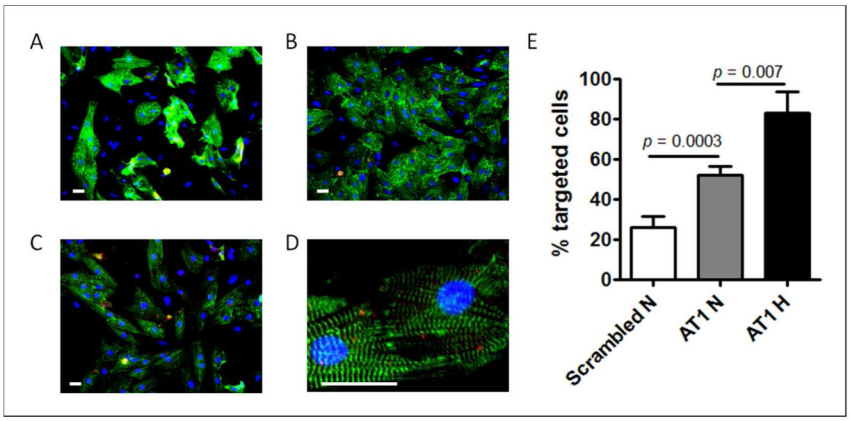

Figure 3.

Cardiac cell targeting in vitro. A. Targeting cardiac cells with nanoparticles conjugated with non-specific scrambled peptide as a targeter. B. Targeting with AT1 nanoparticles. C. Cardiac cells cultured under hypoxic conditions targeted by AT1 nanoparticles. D. Higher magnification of C reveals multiple particles binding to each cell. Sarcomeric actinin (green), nuclei (blue), and nanoparticles (red). Bar= 20 μm in all panels. E. Quantification of % of targeted cells (n≥ 6). Data are means ± SD. 222×108mm (150 × 150 DPI)

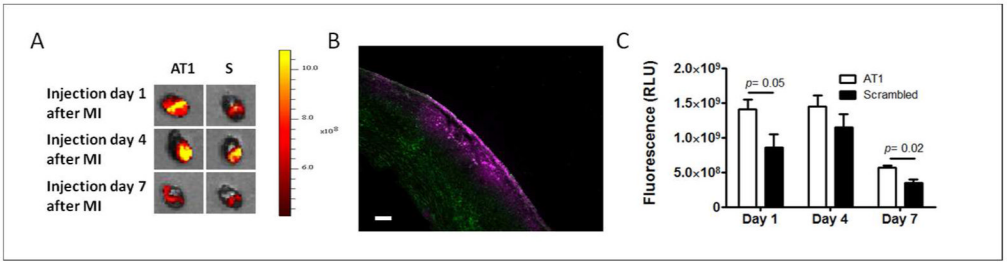

Figure 4.

Targeting the infarcted myocardium. A. IVIS images of hearts injected with AT1 or scrambled (S) nanoparticles 1, 4, and 7 days after infarction. The hearts were isolated 24 h post injection and imaged. LV is located in the lower right side of each image. B. Accumulation of AT1 nanoparticles injected one day post infarction in the LV of the infarcted heart. Nanoparticles: red; tissue auto-fluorescence: green. Bar= 200 μm. C. Quantification of fluorescence in isolated hearts harvested 1 day post injection. 256×66mm (150 × 150 DPI)